Center for Turbulence Research
Proceedings of the Summer Program 2010

Optimal localized control of transitional channel flow

By R. Moarref†, B. K. Lieu†, AND M. R. Jovanović†

For the problem of controlling the onset of turbulence in a channel flow, we study the design of optimal localized state-feedback controllers. The actuation is generated by blowing and suction at the walls, and the actuators are placed along a two-dimensional lattice of equally spaced points with each actuator using information from only a limited number of nearby neighbors. We utilize recently developed tools for designing structured optimal feedback gains to reduce receptivity of velocity fluctuations to flow disturbances in the presence of control. Our preliminary DNS result, conducted at a low Reynolds number, show that this approach can indeed maintain the laminar flow. This is in contrast to the localized strategies obtained by spatial truncation of optimal centralized controllers, which may introduce instability and promote transition even in the situations where the uncontrolled flow stays laminar.

1. Introduction

Feedback strategies for control of fluid flows involve individual system components that are capable of sensing, computation, and actuation. Therefore, an important question in design of flow controllers is related to the interconnection structure between these components. A centralized controller yields best performance at the expense of excessive communication and computation. A fully decentralized controller, while advantageous from a communications perspective, may sacrifice performance. A reasonable compromise between these competing approaches is offered by localized strategies where each component exchanges information with a limited number of nearby components.

Early flow control efforts have focused on drag reduction in turbulent flows. These include the opposition control (Choi *et al.* 1994) and gradient-based strategies where the optimal control problem is solved over infinitesimal (Choi *et al.* 1993; Bewley & Moin 1994) or finite (Bewley *et al.* 2001) time horizons. During the last decade, the emphasis has shifted to model-based techniques from linear control theory which represent an efficient means for design of optimal flow controllers (see Kim & Bewley 2007, for an overview of recent developments). In this paper, we study the problem of controlling the onset of turbulence. Since the early stages of transition are initiated by large flow receptivity (Butler & Farrell 1992; Trefethen *et al.* 1993; Bamieh & Dahleh 2001; Jovanović & Bamieh 2005), we formulate an optimal control problem aimed at reducing this receptivity. For transition control at low Reynolds numbers, this strategy has proven successful in both vibrational sensor-less (Moarref & Jovanović 2010; Lieu *et al.* 2010) and centralized feedback (Högberg *et al.* 2003) setups. These references show that, by

† Department of Electrical and Computer Engineering, University of Minnesota, Minneapolis, MN 55455, USA (mihailo@umn.edu).

substantially reducing large flow receptivity, transition to turbulence can be prevented and even relaminarization of a fully-developed turbulent flow can be achieved.

The main difference between the problem addressed here and by Högberg *et al.* (2003) is that we consider control designs that are localized in space. Namely, the actuation at a certain location depends only on local flow information. The localized controller is obtained using recently developed tools for optimal design of feedback gains subject to structural constraints (Fardad *et al.* 2009; Lin *et al.* 2010). We compare the performance of the optimal localized controller with that of the optimal centralized controller and the controller that is obtained by spatial truncation of the centralized feedback gain. When the actuators use information from only the nearest neighbor components, we demonstrate the danger of enforcing the constraint by spatial truncation. On the other hand, we show that the optimal localized controller achieves performance comparable to that of the optimal centralized controller.

The paper is organized as follows. In § 2, the evolution model for channel flow subject to body force disturbances and boundary actuation is derived. The problem of optimal state-feedback design in the presence of structural constraints is formulated in § 3. In addition, a gradient descent method for solving necessary conditions for optimality is briefly described. In § 4, the effectiveness of the designed feedback gains for controlling the onset of turbulence is examined by comparing the receptivity of the controlled flows and the flow with no control. Our design is further verified using direct numerical simulations of the nonlinear flow dynamics. We conclude the paper in § 5.

2. Problem formulation

2.1. *Governing equations*

We consider an incompressible channel flow, driven by a fixed pressure gradient and subject to a control actuation in the form of blowing and suction along the walls. The evolution of infinitesimal fluctuations around the laminar parabolic profile $U(y)$ is governed by the linearized Navier-Stokes (NS) equations

$$\mathbf{v}_t \;=\; -U\,\mathbf{v}_x - U'\,v_2\,\mathbf{i} \;-\; \boldsymbol{\nabla} p \;+\; (1/R_c)\Delta\mathbf{v} \;+\; \mathbf{d}, \quad 0 \;=\; \boldsymbol{\nabla}\cdot\mathbf{v}, \tag{2.1}$$

where $\mathbf{i}$ denotes the unit vector in the streamwise direction, and $R_c = U_c\,\delta/\nu$ is the Reynolds number defined in terms of the centerline velocity of the parabolic laminar profile U_c and channel half-height δ. The spatial coordinates and time are denoted by (x, y, z) and t, respectively. The kinematic viscosity is denoted by ν, p is the pressure, the velocity fluctuations are given by $\mathbf{v} = (v_1, v_2, v_3)$, and $\mathbf{d} = (d_1, d_2, d_3)$ represents the body force disturbance. Here, the indices 1, 2, and 3 correspond to x, y, and z coordinates, respectively, $\boldsymbol{\nabla}$ is the gradient, $\Delta = \boldsymbol{\nabla}\cdot\boldsymbol{\nabla}$ is the Laplacian, and $U'(y) = \mathrm{d}U(y)/\mathrm{d}y$. Actuation along the walls imposes the following boundary conditions on the wall-normal velocity

$$v_2(x, y \,=\, -1, z, t) \;=\; v_{2,l}(x, z, t), \quad v_2(x, y \,=\, 1, z, t) \;=\; v_{2,u}(x, z, t), \tag{2.2}$$

where $v_{2,l}$ and $v_{2,u}$ denote actuations at the lower and upper walls. The horizontal velocity components satisfy Dirichlet boundary conditions

$$v_1(x, y \,=\, \pm 1, z, t) \;=\; v_3(x, y \,=\, \pm 1, z, t) \;=\; 0.$$

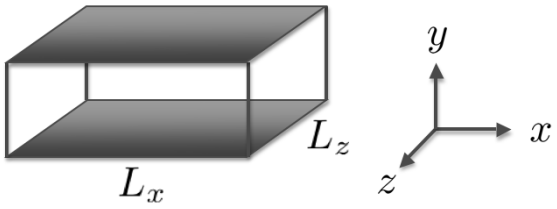

FIGURE 1. A periodic channel with size $L_x \times 2 \times L_z$.

To obtain the standard control formulation, the actuation must enter as an explicit input into the evolution equation (Zhou *et al.* 1996). The following change of variables

$$v_2(x,y,z,t) \;=\; \bar{v}_2(x,y,z,t) \;+\; f_l(y)\, v_{2,l}(x,z,t) \;+\; f_u(y)\, v_{2,u}(x,z,t), \tag{2.3}$$

can be used to achieve this objective, where f_l and f_u are specified by the requirement that $\bar{v}_2$ satisfies Dirichlet and Neumann boundary conditions at the walls:

$$f_l(y) \;=\; \left(y^3 - 3y + 2\right)/4, \quad f_u(y) \;=\; -\left(y^3 - 3y - 2\right)/4.$$

The evolution model for the controlled flow is determined by (see Appendix A for details)

$$\boldsymbol{\phi}_t \;=\; \mathcal{A}\,\boldsymbol{\phi} \;+\; \mathcal{B}_1\,\mathbf{d} \;+\; \mathcal{B}_2\,\mathbf{u}, \quad \mathbf{v} \;=\; \mathcal{C}_1\,\boldsymbol{\phi}, \tag{2.4}$$

where $\boldsymbol{\phi}(x,y,z,t) = [\,\boldsymbol{\phi}_1^T(x,y,z,t) \;\; \boldsymbol{\phi}_2^T(x,z,t)\,]^T$ is the vector of state variables. Here, $\boldsymbol{\phi}_1 = [\,\bar{v}_2 \;\; \eta\,]^T$, where $\eta = v_{1z} - v_{3x}$ denotes the wall-normal vorticity, $\boldsymbol{\phi}_2 = [\,v_{2,l} \;\; v_{2,u}\,]^T$ is the boundary-actuation-vector, and $\mathbf{u} = [\,u_1 \;\; u_2\,]^T = \boldsymbol{\phi}_{2t}$ is the control input to the evolution model. The operator $\mathcal{A}$ represents the dynamical generator of Eq. (2.4), $\mathcal{B}_1$ and $\mathcal{B}_2$ determine how disturbances and control enter into Eq. (2.4), and $\mathcal{C}_1$ specifies the kinematic relation between velocity fluctuations $\mathbf{v}$ and state $\boldsymbol{\phi}$. The definitions of these operators are provided in Appendix A.

2.2. *Actuation along the discrete lattice*

In what follows, we impose periodic boundary conditions in the horizontal directions; see Fig. 1 for geometry. The size of the computational domain is given by $L_x \times 2 \times L_z$, where L_x and L_z denote the channel lengths in x and z. We use N_x and N_z Fourier modes to represent differential operators in the streamwise and spanwise directions, respectively. In physical space, this yields a two-dimensional lattice of equally-spaced points ($x_r = rh_x$, $z_s = sh_z$), with $r \in \mathbb{N}_x = \{0, 1, \ldots, N_x - 1\}$ and $s \in \mathbb{N}_z = \{0, 1, \ldots, N_z - 1\}$. The horizontal spacings between two adjacent points are determined by $h_x = L_x/N_x$ and $h_z = L_z/N_z$. For simplicity, we use the same symbols to denote variables in physical and frequency domains; for example, $v_2(m,n;y,t)$ denotes the frequency representation of $v_2(r,s;y,t) = v_2(x_r,y,z_s,t)$, where $m \in \mathbb{Z}_x = \{-N_x/2, -N_x/2+1, \ldots, N_x/2-1\}$ and $n \in \mathbb{Z}_z = \{-N_z/2, -N_z/2+1, \ldots, N_z/2-1\}$. The corresponding spatial wavenumbers are determined by $k_m = m\,2\pi/L_x$ and $k_n = n\,2\pi/L_z$.

We consider the design problem with wall-actuation taking place along the aforementioned two-dimensional lattice. Furthermore, we assume that the states are available for measurement, implying that the control input at (x_r, z_s) is obtained from

$$\begin{aligned}\mathbf{u}(r,s;t) \;=\; -\sum_{\tilde{r}\in\mathbb{N}_x,\,\tilde{s}\in\mathbb{N}_z} \Bigg(\int_{-1}^{1} \mathcal{K}_1(r-\tilde{r}, s-\tilde{s}; y)\,\boldsymbol{\phi}_1(\tilde{r},\tilde{s};y,t)\,\mathrm{d}y \;+ \\ \mathcal{K}_2(r-\tilde{r}, s-\tilde{s})\,\boldsymbol{\phi}_2(\tilde{r},\tilde{s};t)\Bigg),\end{aligned} \tag{2.5}$$

where $\mathcal{K}_1$ and $\mathcal{K}_2$ are the corresponding state-feedback gains. The frequency representation of Eq. (2.5), for each $m \in \mathbb{Z}_x$ and $n \in \mathbb{Z}_z$, is given by

$$\mathbf{u}(m,n;t) \;=\; -\int_{-1}^{1} \mathcal{K}_1(m,n;y)\,\boldsymbol{\phi}_1(m,n;y,t)\,\mathrm{d}y \;-\; \mathcal{K}_2(m,n)\,\boldsymbol{\phi}_2(m,n;t). \tag{2.6}$$

For computational purposes, the wall-normal operators in Eqs. (2.4) and (2.6) are approximated using pseudospectral method with N_y Chebyshev collocation points (Weideman & Reddy 2000). This yields the discretized evolution model

$$\begin{aligned} \dot{\boldsymbol{\phi}}_{m,n}(t) \;&=\; A_{m,n}\,\boldsymbol{\phi}_{m,n}(t) \,+\, B_{1m,n}\,\mathbf{d}_{m,n}(t) \,+\, B_{2m,n}\,\mathbf{u}_{m,n}(t), \\ \mathbf{v}_{m,n}(t) \;&=\; C_{1m,n}\,\boldsymbol{\phi}_{m,n}(t), \end{aligned} \tag{2.7}$$

parameterized by $m \in \mathbb{Z}_x$ and $n \in \mathbb{Z}_z$. Here, $\boldsymbol{\phi}_{m,n}(t)$ and $\mathbf{u}_{m,n}(t)$ are column-vectors with $(2N_y+2)$ and 2 components, respectively, and the dot is the derivative with respect to time. Furthermore, the control action is determined by

$$\mathbf{u}_{m,n}(t) \;=\; -K_{m,n}\,\boldsymbol{\phi}_{m,n}(t) \;=\; -\begin{bmatrix} K_{1m,n} & K_{2m,n} \end{bmatrix} \begin{bmatrix} \boldsymbol{\phi}_{1m,n}(t) \\ \boldsymbol{\phi}_{2m,n}(t) \end{bmatrix} \tag{2.8}$$

where the $2 \times (2N_y+2)$ matrix $K_{m,n}$ denotes the discretized form of the state-feedback gain in the frequency domain.

3. Design of optimal localized feedback gains

We consider the problem of designing structured optimal feedback gains for controlling the onset of turbulence. To this end, we determine the stabilizing gains that minimize a performance index J obtained by penalizing flow receptivity and control effort. These are, respectively, quantified by the variance amplification of velocity fluctuations $\mathbf{v}$ in the presence of zero-mean white stochastic disturbance $\mathbf{d}$, and by the kinetic energy of the blowing and suction along the walls. In addition, to obtain the well-posed optimal control formulation, the penalty on $\mathbf{u}$ is introduced in the performance index as well.

The above described optimal control problem amounts to finding the stabilizing gains that minimize the variance amplification of the performance output

$$\boldsymbol{\zeta}_{m,n}(t) \;=\; \begin{bmatrix} W^{1/2}\,C_{1m,n} \\ 0 \end{bmatrix} \boldsymbol{\phi}_{m,n}(t) \,+\, \begin{bmatrix} 0 \\ R^{1/2} \end{bmatrix} \mathbf{u}_{m,n}(t). \tag{3.1}$$

Here, R is the positive definite matrix, and W denotes a $3N_y \times 3N_y$ diagonal matrix with $\{\mathbf{w},\mathbf{w},\mathbf{w}\}$ on its main diagonal where the vector $\mathbf{w}$ contains the integration weights at the Chebyshev collocation points (Hanifi *et al.* 1996). Substitution of Eq. (2.8) into Eqs. (2.7) and (3.1) yields the following evolution model of the closed-loop system

$$\begin{aligned} \dot{\boldsymbol{\phi}}_{m,n}(t) \;&=\; \left(A_{m,n} \,-\, B_{2m,n}\,K_{m,n}\right) \boldsymbol{\phi}_{m,n}(t) \,+\, B_{1m,n}\,\mathbf{d}_{m,n}(t), \\ \boldsymbol{\zeta}_{m,n}(t) \;&=\; \begin{bmatrix} W^{1/2}\,C_{1m,n} \\ -R^{1/2}\,K_{m,n} \end{bmatrix} \boldsymbol{\phi}_{m,n}(t). \end{aligned} \tag{3.2}$$

Mathematically, the problem of steady-state variance (i.e., the $\mathcal{H}_2$ norm) minimization for system given by Eq. (3.2), can be formulated as (Zhou *et al.* 1996)

$$\text{minimize}: \;\; J(K) \;=\; \sum_{m\in\mathbb{Z}_x, n\in\mathbb{Z}_z} \text{trace}\left(X_{m,n}\,Q_{Bm,n}\right), \tag{3.3a}$$

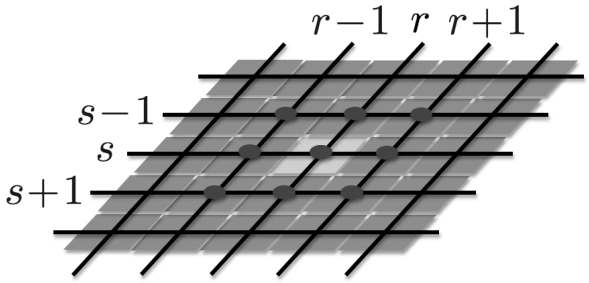

FIGURE 2. Sketch of a localized control strategy where the actuator placed at (r, s) uses information from only the nearest neighbors on the two-dimensional lattice.

$$\text{subject to}: \; A^*_{\mathrm{cl}m,n}\, X_{m,n} + X_{m,n}\, A_{\mathrm{cl}m,n} \;=\; -\big(Q_{Cm,n} \;+\; K^*_{m,n}\, R\, K_{m,n}\big), \qquad (3.3b)$$

where * denotes the complex conjugate transpose, $A_{\mathrm{cl}m,n} = A_{m,n} - B_{2m,n} K_{m,n}$, $Q_{Bm,n} = B_{1m,n} W^{-1} B^*_{1m,n}$, and $Q_{Cm,n} = C^*_{1m,n} W C_{1m,n}$. The solution to Eq. (3.3) in the absence of structural constraints is given by

$$K_{m,n} \;=\; R^{-1}\, B^*_{2m,n}\, X_{m,n}, \qquad (3.4)$$

where $X_{m,n}$ is determined from the algebraic Riccati equation

$$A^*_{m,n}\, X_{m,n} \;+\; X_{m,n}\, A_{m,n} \;-\; X_{m,n}\, B_{2m,n}\, R^{-1}\, B^*_{2m,n}\, X_{m,n} \;+\; Q_{Cm,n} \;=\; 0.$$

In general, actuation based on the optimal solution given by Eq. (3.4), necessitates centralized implementation that requires knowledge of the entire flow field. The problem of designing optimal centralized feedback gains for controlling transition is considered by Högberg *et al.* (2003). As shown by Bamieh *et al.* (2002), the magnitude of the centralized feedback gains decays exponentially in space, implying that they can be spatially truncated. Although this suggests a way for obtaining localized controllers, the problem of designing optimal localized feedback gains is more challenging. The main difference between the problem considered here and in Högberg *et al.* (2003) is that we ask the following question: Can actuation based on local flow information prevent transition to turbulence? To answer this, we a priori impose structural constraints on the feedback gains. It is assumed that each actuator uses information only from the points that are located within a small relative distance. The set of all such relative distances in units of h_x and h_z is denoted by S. In other words, only the feedback gains that correspond to the points in S are allowed to be nonzero. For example, when information from only the nearest neighbors is used, we have (see Fig. 2 for an illustration)

$$S \;=\; \big\{(r,s) \;\big|\; r = \{-1,0,1\}, s = \{-1,0,1\}\big\}\,.$$

Furthermore, by $F(r, s)$ we denote the corresponding structured feedback gains.

For spatially invariant systems, the structured optimal state-feedback problem can be formulated as (Fardad *et al.* 2009)

$$\text{minimize}: \; J(F) \;=\; \sum_{m\in\mathbb{Z}_x, n\in\mathbb{Z}_z} \mathrm{trace}\,\left(X_{m,n}\, Q_{Bm,n}\right), \qquad \text{(P1)}$$

$$\text{subject to}: \; A^*_{\mathrm{cl}m,n}\, X_{m,n} + X_{m,n}\, A_{\mathrm{cl}m,n} \;=\; -\big(Q_{Cm,n} \;+\; C^*_{2m,n}\, F^*\, R\, F\, C_{2m,n}\big), \quad \text{(P2)}$$

where F denotes the block-row matrix, which is independent of m and n, and contains

the structured feedback gain $F(r,s)$,

$$F \;=\; \mathrm{row}\,\{F(r,s)\}_{(r,s)\in S}\,, \tag{P3}$$

and $C_{2m,n}$ is given by the block-column matrix

$$C_{2m,n} \;=\; \mathrm{col}\left\{\mathrm{e}^{-\mathrm{i}\,2\pi\,(r\,m/N_x\,+\,s\,n/N_z)}\,I\right\}_{(r,s)\in S}. \tag{P4}$$

Here, I is the identity matrix of size $2N_y+2$, and $A_{\mathrm{cl}m,n} = A_{m,n} - B_{2m,n}\,F\,C_{2m,n}$ denotes the dynamical generator of the closed-loop system.

Note that in the absence of structural constraints (i.e., $S = \mathbb{N}_x \times \mathbb{N}_z = \{(r,s)\big|\; r \in N_x, s \in N_z\}$), the structured optimal control problem (P1)-(P4) reduces to the unstructured problem given by Eq. (3.3).

3.1. *Computation of the structured optimal feedback gains*

We briefly describe the method that is used to solve the optimal control problem (P1)-(P4) with specified S. This method is adopted from the developments of Lin *et al.* (2010), where efficient descent methods for structured optimal design are introduced.

The necessary conditions for optimality of the stabilizing feedback gain F with $R = rI_{2\times 2}$ in (P2), $r>0$, are given by (Lin *et al.* 2010)

$$\begin{aligned}
A^*_{\mathrm{cl}m,n}\,X_{m,n} \,+\, X_{m,n}\,A_{\mathrm{cl}m,n} \;&=\; -\left(Q_{Cm,n} \,+\, r\,C^*_{2m,n}\,F^*\,F\,C_{2m,n}\right),\\
A_{\mathrm{cl}m,n}\,Y_{m,n} \,+\, Y_{m,n}\,A^*_{\mathrm{cl}m,n} \;&=\; -\,Q_{Bm,n},\\
F \;=\; \frac{1}{r}\left(\sum_{m\,\in\,\mathbb{Z}_x,\,n\,\in\,\mathbb{Z}_z} B^*_{2m,n}\,X_{m,n}\,Y_{m,n}\,C^*_{2m,n}\right)&\left(\sum_{m\,\in\,\mathbb{Z}_x,\,n\,\in\,\mathbb{Z}_z} C_{2m,n}\,Y_{m,n}\,C^*_{2m,n}\right)^{-1}.
\end{aligned} \tag{3.5}$$

This system of equations is nonlinear in the unknown matrices $X_{m,n}$, $Y_{m,n}$, and F. Moreover, as seen from the last condition in Eq. (3.5), the structural constraints on F introduce coupling between all wavenumbers; this is in contrast to the unstructured optimal control problem given by Eq. (3.3).

Next, we describe the algorithm that is employed for solving Eq. (3.5) (Lin *et al.* 2010):

Descent method for solving Eq. (3.5):

given stabilizing F^0 that satisfies the structural constraints imposed by S,

for $i = 0, 1, 2, \ldots$, **do:**

(1) compute descent direction $\tilde{F}^i$;

(2) determine step-size q^i;

(3) update $F^{i+1} = F^i + q^i\,\tilde{F}^i$;

until the stopping criterion $||\nabla J(F^i)||_F < \epsilon$ is achieved, where $||\cdot||_F$ denotes the Frobenius norm and ϵ is the convergence tolerance.

We consider the gradient descent direction that provides linear rate of convergence to the local minimum. More sophisticated descent directions, such as Newton or quasi-Newton directions, provide faster convergence at the expense of increased computational cost (for example, see Lin *et al.* 2010). The gradient direction is given by $\tilde{F}^i = -\nabla J(F^i)$ where $\nabla J(F^i)$ is determined from (Lin *et al.* 2010)

$$\nabla J(F^i) \;=\; \frac{2}{N_x\,N_z} \sum_{m\,\in\,\mathbb{Z}_x,\,n\,\in\,\mathbb{Z}_z} \left(r\,F\,C_{2m,n} \,-\, B^*_{2m,n}\,X_{m,n}\right) Y_{m,n}\,C^*_{2m,n}.$$

For the step-size rule, the backtracking line search (Boyd & Vandenberghe 2004) is used where in addition to guaranteeing descent of the performance index, we also guarantee

the stability of the updated closed-loop system. Namely, we repeat $q^i = \beta q^i$ $(0 < \beta < 1)$ until both of the following conditions are satisfied:

(a) descent: $J(F^i + q^i \tilde{F}^i) < J(F^i) + \alpha q^i \sum_{m,n} (\nabla J(F^i)^T \tilde{F}^i)$ with $0 < \alpha < 0.5$;

(b) closed-loop stability: $A_{m,n} - B_{2m,n} F C_{2m,n}$ is stable for all $m \in \mathbb{Z}_x$ and $n \in \mathbb{Z}_z$.

4. Localized control of transition

As discussed in § 1, the problem of controlling the onset of turbulence is formulated as the receptivity (i.e., the $\mathcal{H}_2$ norm) reduction problem. Therefore, to assess the effectiveness of feedback controllers, we compare the receptivity of controlled flows to the receptivity of flow with no control. We consider the stochastically forced linearized NS equations in the subcritical regime where the flow with no control is linearly stable. The energy density of fluctuations in the presence of stochastic forcing is used to quantify the flow receptivity. The zero-mean stochastic forcing which is white in time and y, and purely harmonic in horizontal directions, yields a nonzero steady-state variance of velocity fluctuations $E(k_m, k_n)$ (Farrell & Ioannou 1993). For any $m \in \mathbb{Z}_x$ and $n \in \mathbb{Z}_z$, this quantity can be obtained from

$$\begin{gathered} E(k_m, k_n) \;=\; \text{trace}\,(Z_{m,n}\, Q_{Bm,n})\,, \\ (A_{m,n} - B_{2m,n}\, F\, C_{2m,n})^*\, Z_{m,n} \;+\; Z_{m,n}\,(A_{m,n} - B_{2m,n}\, F\, C_{2m,n}) \;=\; -Q_{Cm,n}. \end{gathered} \tag{4.1}$$

For the flow with no control (i.e., for $F = 0$), the streamwise-constant fluctuations are the most amplified by the linearized dynamics (Farrell & Ioannou 1993; Bamieh & Dahleh 2001; Jovanović & Bamieh 2005). These fluctuations correspond to the streamwise streaks that are ubiquitous in wall-bounded shear flows. The large amplification of streaks is physically associated with the vortex-tilting (lift-up) mechanism that arises from the non-normal coupling between dynamics of the wall-normal velocity and vorticity fluctuations (Butler & Farrell 1992; Reddy & Henningson 1993). This non-normal coupling is also responsible for the pseudo-resonance phenomenon (Trefethen *et al.* 1993; Schmid 2007) where large amplification of harmonic disturbances, which are not associated with eigenvalues of the linearized model, is obtained. On the other hand, the least stable modes of the uncontrolled flow, i.e., the Tollmien-Schlichting (TS) waves, are much less amplified than the streamwise streaks. This highlights the importance of amplification of the streamwise constant fluctuations in the early stages of transition. Therefore, a control strategy that is capable of reducing the receptivity of streamwise streaks to stochastic disturbances represents a viable approach for controlling the onset of turbulence.

4.1. *Receptivity of the controlled flows*

For the controlled flows, we consider three state-feedback gains: (a) the centralized gains determined by Eq. (3.4); (b) the truncated gains obtained by enforcing the structural constraints by spatial truncation of the centralized feedback gains; and (c) the optimal localized gain F that is designed using the method presented in § 3.1. For the truncated and localized controllers, we consider the case where each actuator uses information from only its nearest neighbors (for an illustration, see Fig. 2).

Fig. 3 compares the energy amplification of the controlled flows with $R_c = 2000$ and the flow with no control for different horizontal wavenumbers. The optimal centralized controller significantly reduces flow receptivity for all wavenumbers. Compared with the flow with no control, an 89% reduction in amplification of the most energetic structures (i.e., streaks) is achieved (cf. peak values in Fig. 3(a)).

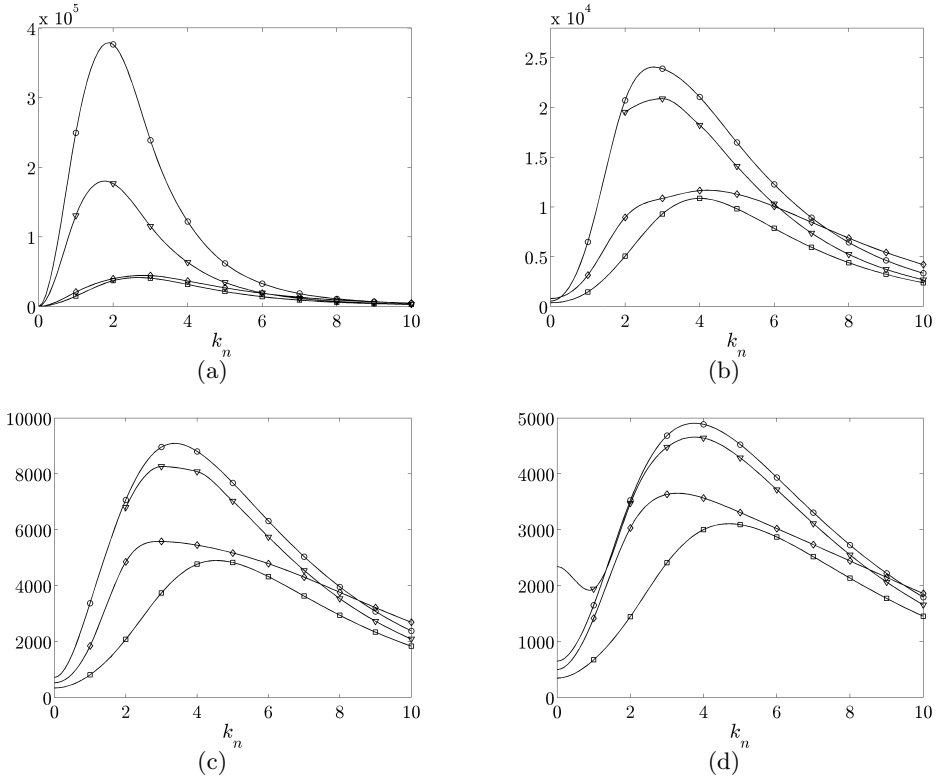

FIGURE 3. Energy density of the velocity fluctuations $E(k_n)$ for the uncontrolled flow with $R_c = 2000$ ($\circ$), optimal centralized ($\square$), truncated centralized ($\triangledown$), and optimal localized ($\diamond$) controllers for (a) $k_m = 0$; (b) $k_m = 0.5$; (c) $k_m = 1$; and (d) $k_m = 1.5$. The truncated controller is unstable for $k_m = \{0.5, 1\}$ and $k_n = \{0, 1\}$ and the energy density is not defined for any combination of these wavenumbers. Note: The energy density is computed at the discrete set of wavenumbers k_n and k_m (symbols) and the lines are plotted for visual aid.

Next, we look at the flows that are controlled by the truncated centralized and optimal localized feedback gains. Figures 3(b) and 3(c) illustrate that truncated centralized gains introduce instability at small streamwise wavenumbers. The numerical simulations of § 4.2 confirm that the flow controlled with these gains diverges from the laminar profile and becomes turbulent. In addition, for the stable wavenumbers, Fig. 3 shows that the variance amplification of the truncated centralized controller is much larger than that of the centralized controller. This justifies the need for designing optimal localized controllers that satisfy the structural constraints and exhibit similar performance to that of the centralized controller.

In order to obtain the optimal localized gains, we have used the truncated centralized gains to initialize the iterative scheme described in § 3.1. Although the truncated gains are not stabilizing, it turns out that the initial gradient direction can be used to obtain stabilizing structured gains. We are currently also developing algorithms based on the augmented Lagrangian method (Lin *et al.* 2010) that does not require stabilizing gains for the initial iteration.

Figure 3 shows that the optimal localized gains maintain stability for all wavenumbers. In addition, the variance amplification of the localized controller is similar to that of

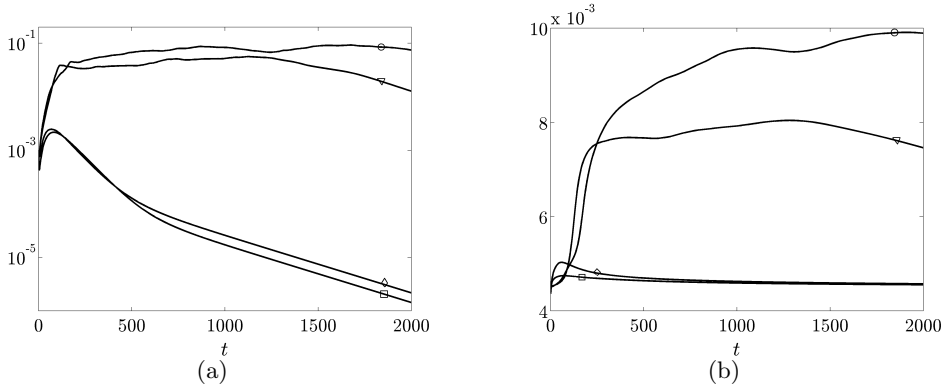

FIGURE 4. (a) Energy of the velocity fluctuations $E(t)$; and (b) skin-friction drag coefficient $C_f(t)$ for the flow with no control ($\circ$) and optimal centralized ($\square$), truncated centralized ($\triangledown$), and optimal localized ($\diamond$) controllers. The results are obtained using DNS with $R_c = 2000$.

the centralized controller. In particular, Fig. 3(a) shows that amplification of the most energetic modes is almost the same for optimal localized and centralized controllers. Therefore, the properly designed localized controller is a good candidate for controlling the onset of turbulence, as verified in direct numerical simulations of § 4.2.

4.2. *Direct numerical simulations*

We simulate a channel flow with $R_c = 2000$ that is driven by a constant pressure gradient and is subject to actuation in the form of blowing and suction at the walls. This value of R_c is smaller than the Reynolds number at which linear instability occurs ($R_c = 5772$) and larger than the value for which transition usually takes place in experiments and DNS ($R_c \approx 1000$). The fully nonlinear NS equations are discretized with spectral accuracy using Fourier modes in horizontal directions and Chebyshev polynomials in y, as described in § 2.2. The lengths of the computational box in units of the channel half-height δ are $L_x = 4\pi$ and $L_z = 2\pi$, with $N_x \times N_y \times N_z = 52 \times 97 \times 42$ points in x, y, and z directions (after dealiasing in x and z). In our study, 42 collocation points in y were enough for computing convergent feedback gains. These gains are then interpolated and scaled to determine the feedback gains for 97 Chebyshev collocation points.

The flow is initialized with a perturbation that is capable of driving the uncontrolled flow to turbulence. For the optimal centralized, truncated optimal centralized, and optimal localized feedback gains, we evaluate the energy of velocity fluctuations $E(t)$ around the laminar parabolic profile and the skin-friction drag coefficient $C_f(t)$.

Figure 4(a) shows $E(t)$ for the controlled flows and the flow with no control. Compared with its initial value, the energy of three-dimensional fluctuations in the uncontrolled flow is increased by approximately two orders of magnitude, resulting in divergence from the laminar parabolic profile. On the other hand, the optimal centralized controller provides decay of fluctuations' energy to zero after a small transient growth. Our results agree with the study of Högberg *et al.* (2003) where it was shown that the optimal centralized controller is capable of preventing transition. The truncated centralized controller introduces faster growth of $E(t)$ relative to the flow with no control, thereby promoting divergence from the laminar flow. On the other hand, Fig. 4(a) shows that the optimal localized controller is capable of maintaining the laminar flow by providing performance comparable to that of the optimal centralized controller.

Figure 4(b) shows the skin-friction drag coefficient $C_f(t)$. We see that the drag coefficients of the optimal centralized and localized controllers are equal to 4.5×10^{-3}, which corresponds to the drag coefficient of the laminar flow. On the other hand, the drag coefficient of the uncontrolled flow is 10^{-2}, which is a clear indicator of a fully developed turbulent flow. The drag coefficient of the truncated centralized controller is approximately 7.5×10^{-3}. This suggests that although the truncated gains cannot maintain the laminar flow, they achieve 16% reduction in drag relative to the uncontrolled turbulent flow.

5. Concluding remarks

We consider design of optimal localized flow controllers for preventing transition to turbulence. We formulate an optimal control problem for minimizing the flow receptivity and control effort. In addition, structural constraints are imposed on the feedback gains such that only the gains that are associated with the nearest neighbors are nonzero. This problem is solved using recently developed techniques for optimal design of state-feedback controllers with structural constraints. We show that spatial truncation of the optimal centralized gains can introduce flow instability. Therefore, the truncated feedback gains may not be suitable for controlling transition, and they may even promote turbulence in the situations where the uncontrolled flow stays laminar. On the other hand, we demonstrate that the optimal localized controller can exhibit receptivity reduction similar to that of the optimal centralized controller. Furthermore, our simulations of the nonlinear flow dynamics show that transition can be prevented using optimal localized gains.

Acknowledgments

Part of this work was performed during the 2010 Center for Turbulence Research Summer Program with financial support from Stanford University and NASA Ames Research Center. We would like to thank Prof. P. Moin for stimulating discussions and his interest in our work, Dr. J. Larsson for his hospitality during the stay, and Dr. J. W. Nichols for his useful comments that helped us improve quality of our presentation. Financial support from the National Science Foundation under CAREER Award CMMI-06-44793 is gratefully acknowledged.

Appendix A. Evolution model with forcing and actuation along the walls

The evolution model given by Eq. (2.4), is obtained from Eq. (2.1) by eliminating pressure via a standard choice of wall-normal velocity and vorticity (v, η) as the flow variables. By incorporating the change of variables introduced by Eq. (2.3), and augmenting the flow variables by the boundary actuation, we obtain the state vector $\boldsymbol{\phi} = [\,\boldsymbol{\phi}_1^T \;\; \boldsymbol{\phi}_2^T\,]^T$ with $\boldsymbol{\phi}_1 = [\,\bar{v}_2 \;\; \eta\,]^T$ and $\boldsymbol{\phi}_2 = [\,v_{2,l} \;\; v_{2,u}\,]^T$. This choice brings the time-derivative of the boundary actuation $\mathbf{u} = \boldsymbol{\phi}_{2t}$ as an explicit input to the evolution model. The operators in the evolution model are determined by

$$\mathcal{A} = \begin{bmatrix} \mathcal{A}_{11} & \mathcal{A}_{12} \\ 0 & 0 \end{bmatrix},\; \mathcal{B}_1 = \begin{bmatrix} \mathcal{B}_{11} \\ 0 \end{bmatrix},\; \mathcal{B}_2 = \begin{bmatrix} \mathcal{B}_{21} \\ \mathcal{B}_{22} \end{bmatrix},\; \mathcal{C}_1 = \begin{bmatrix} \mathcal{C}_{11} & \mathcal{C}_{12} \end{bmatrix},$$

where

$$\mathcal{A}_{11} = \begin{bmatrix} \Delta^{-1}\left((1/R_c)\Delta^2 - (U_0\Delta - U_0'')\,\partial_x\right) & 0 \\ -U_0'\,\partial_z & (1/R_c)\Delta - U_0\,\partial_x \end{bmatrix},$$

$$\mathcal{A}_{12} = \begin{bmatrix} \mathcal{A}_{12,1} & \mathcal{A}_{12,2} \\ -U_0' f_l\,\partial_z & -U_0' f_u \partial_z \end{bmatrix},$$

$$\mathcal{A}_{12,1} = \Delta^{-1}((2\,f_l''(\partial_x^2+\partial_z^2) + f_l(\partial_x^2+\partial_z^2)^2)/R_c - (U_0 f_l'' + U_0 f_l(\partial_x^2+\partial_z^2) - U_0'' f_l)\,\partial_x),$$

$$\mathcal{A}_{12,2} = \Delta^{-1}((2\,f_u''(\partial_x^2+\partial_z^2) + f_u(\partial_x^2+\partial_z^2)^2)/R_c - (U_0 f_u'' + U_0 f_u(\partial_x^2+\partial_z^2) - U_0'' f_u)\,\partial_x),$$

$$\mathcal{B}_{11} = \begin{bmatrix} \Delta^{-1}(-\partial_{xy}) & \Delta^{-1}(\partial_x^2+\partial_z^2) & \Delta^{-1}(-\partial_{yz}) \\ \partial_z & 0 & -\partial_x \end{bmatrix},$$

$$\mathcal{B}_{21} = \begin{bmatrix} \Delta^{-1}(-f_l'' - f_l(\partial_x^2+\partial_z^2)) & \Delta^{-1}(-f_u'' - f_u(\partial_x^2+\partial_z^2)) \\ 0 & 0 \end{bmatrix},\ \mathcal{B}_{22} = \begin{bmatrix} 1 & 0 \\ 0 & 1 \end{bmatrix},$$

$$\mathcal{C}_{11} = \begin{bmatrix} -\partial_{xy}(\partial_x^2+\partial_z^2)^{-1} & \partial_z(\partial_x^2+\partial_z^2)^{-1} \\ I & 0 \\ -\partial_{yz}(\partial_x^2+\partial_z^2)^{-1} & -\partial_x(\partial_x^2+\partial_z^2)^{-1} \end{bmatrix},$$

$$\mathcal{C}_{12} = \begin{bmatrix} -f_l'\,\partial_x(\partial_x^2+\partial_z^2)^{-1} & -f_u'\,\partial_x(\partial_x^2+\partial_z^2)^{-1} \\ f_l & f_u \\ -f_l'\,\partial_z(\partial_x^2+\partial_z^2)^{-1} & -f_u'\,\partial_z(\partial_x^2+\partial_z^2)^{-1} \end{bmatrix},$$

with $\Delta = \partial_x^2 + \partial_y^2 + \partial_z^2$ denoting the three-dimensional Laplacian.

REFERENCES

Bamieh, B. & Dahleh, M. 2001 Energy amplification in channel flows with stochastic excitation. *Phys. Fluids* **13** (11), 3258–3269.

Bamieh, B., Paganini, F. & Dahleh, M. A. 2002 Distributed control of spatially invariant systems. *IEEE Trans. Automat. Control* **47** (7), 1091–1107.

Bewley, T. & Moin, P. 1994 Optimal control of turbulent channel flows. *Active Control of Vibration and Noise, ASME-DE* **75**.

Bewley, T., Moin, P. & Temam, R. 2001 DNS-based predictive control of turbulence: an optimal benchmark for feedback algorithms. *J. Fluid Mech.* **447**, 179–225.

Boyd, S. & Vandenberghe, L. 2004 *Convex optimization*. New York: Cambridge University Press.

Butler, K. M. & Farrell, B. F. 1992 Three-dimensional optimal perturbations in viscous shear flow. *Phys. Fluids A* **4**, 1637.

Choi, H., Moin, P. & Kim, J. 1994 Active turbulence control for drag reduction in wall-bounded flows. *J. Fluid Mech.* **262**, 75–110.

Choi, H., Temam, R., Moin, P. & Kim, J. 1993 Feedback control for unsteady flow and its application to the stochastic Burgers equation. *J. Fluid Mech.* **253**, 509–543.

Fardad, M., Lin, F. & Jovanović, M. R. 2009 On the optimal design of structured feedback gains for interconnected systems. In *Proceedings of the 48th IEEE Conference on Decision and Control*, pp. 978–983. Shanghai, China.

Farrell, B. F. & Ioannou, P. J. 1993 Stochastic forcing of the linearized Navier-Stokes equations. *Phys. Fluids A* **5** (11), 2600–2609.

Hanifi, A., Schmid, P. & Henningson, D. 1996 Transient growth in compressible boundary layer flow. *Phys. Fluids* **8** (3), 826–837.

Högberg, M., Bewley, T. R. & Henningson, D. S. 2003 Linear feedback control and estimation of transition in plane channel flow. *J. Fluid Mech.* **481**, 149–175.

Jovanović, M. R. & Bamieh, B. 2005 Componentwise energy amplification in channel flows. *J. Fluid Mech.* **534**, 145–183.

Kim, J. & Bewley, T. R. 2007 A linear systems approach to flow control. *Annu. Rev. Fluid Mech.* **39**, 383–417.

Lieu, B. K., Moarref, R. & Jovanović, M. R. 2010 Controlling the onset of turbulence by streamwise traveling waves. Part 2: Direct numerical simulations. *J. Fluid Mech.* **663**, 100–119.

Lin, F., Fardad, M. & Jovanović, M. R. 2010 Design of structured optimal feedback gains for large-scale interconnected systems. *IEEE Trans. Automat. Control* Submitted.

Moarref, R. & Jovanović, M. R. 2010 Controlling the onset of turbulence by streamwise traveling waves. Part 1: Receptivity analysis. *J. Fluid Mech.* **663**, 70–99.

Reddy, S. C. & Henningson, D. S. 1993 Energy growth in viscous channel flows. *J. Fluid Mech.* **252**, 209–238.

Schmid, P. J. 2007 Nonmodal stability theory. *Annu. Rev. Fluid Mech.* **39**, 129–162.

Trefethen, L. N., Trefethen, A. E., Reddy, S. C. & Driscoll, T. A. 1993 Hydrodynamic stability without eigenvalues. *Science* **261**, 578–584.

Weideman, J. A. C. & Reddy, S. C. 2000 A MATLAB differentiation matrix suite. *ACM Transactions on Mathematical Software* **26** (4), 465–519.

Zhou, K., Doyle, J. C. & Glover, K. 1996 *Robust and Optimal Control*. Prentice Hall.